

M. Mostafa\*, H. M. Saber, A. A. El-Sadek, and M. Y. Nassar

# Preparation and performance of $^{99}\text{Mo}/^{99\text{m}}\text{Tc}$ chromatographic column generator based on zirconium molybdsilicate

DOI 10.1515/ract-2015-2488

Received July 24, 2015; accepted October 26, 2015; published online December 23, 2015

**Abstract:** Zirconium molybdsilicate (ZrMoSi) gel prepared using  $^{99}\text{Mo}$  radiotracer via peroxy route was used as a base material for  $^{99}\text{Mo}/^{99\text{m}}\text{Tc}$  column generator. The  $^{99\text{m}}\text{Tc}$  elution yield and  $^{99}\text{Mo}$  breakthrough in the eluate were studied as a function of the pH-value of gel precipitation, gel drying temperature and Zr : Mo : Si molar ratio. Precipitation pH-value of 2, drying temperature of 100 °C and Zr : Mo : Si molar ratio of 0.5 : 0.5 : 1 were found to be the optimum conditions achieving  $^{99\text{m}}\text{Tc}$  elution yield of 82% and  $^{99}\text{Mo}$  breakthrough of  $1.0 \times 10^{-3}\%$ . The gel prepared with the optimum conditions was characterized by BET surface area and pore size analyzer, IR spectroscopy, thermal analysis (TGA and DTA), XRD, XRF and FESEM. Technetium-99m eluted from the optimum ZrMoSi  $^{99}\text{Mo}/^{99\text{m}}\text{Tc}$  generator was found to have a high radiochemical purity (98% as  $^{99\text{m}}\text{TcO}_4^-$ ) and chemical purity meeting criteria of clinical grade.

**Keywords:** Zirconium molybdsilicate,  $^{99}\text{Mo}/^{99\text{m}}\text{Tc}$  generator, characterization, performance, elution, radionuclidic purity, radiochemical purity.

## 1 Introduction

$^{99\text{m}}\text{Tc}$  ( $t_{1/2} = 6.01$  h) is a key isotope used in nuclear imaging processes accounting for more than 80% of nuclear medicine procedures. It is the most common radiotracer used for single photon emission computed tomography (SPECT), emitting 140 keV gamma-rays. For example,

a bone scan can be carried out with planar camera with  $^{99\text{m}}\text{Tc}-\text{MDP}$ , while a cardiac scan can be performed with a SPECT camera and  $^{99\text{m}}\text{Tc}-\text{sestamibi}$  [1].

Technetium-99m is the decay product of  $^{99}\text{Mo}$  ( $t_{1/2} = 65.94$  h), which can be, in turn, produced from nuclear reactors via  $^{235}\text{U}(n, f)^{99}\text{Mo}$  and  $^{98}\text{Mo}(n, \gamma)^{99}\text{Mo}$  or from cyclotrons via  $^{100}\text{Mo}(p, 2n)^{99}\text{Mo}$  [2]. Technetium-99m is mainly supplied from  $^{99}\text{Mo}/^{99\text{m}}\text{Tc}$  chromatographic column generators based on alumina loaded with fission- $^{99}\text{Mo}$  (with a loading capacity of 2 mg Mo/g at pH 5–6.2) [3]. In addition, hydrous zirconium oxide, hydrous titanium oxide, manganese dioxide, silica gel and hydroaluminates have also been investigated as base column beds for fission  $^{99}\text{Mo}/^{99\text{m}}\text{Tc}$  generators [4].

Molybdenum-99 produced from nuclear reactors via the fission route is advantageous because of its high specific activity of the order of tens thousands of Ci g<sup>-1</sup> while it has the shortcomings of the requirement of highly expensive hot cells with sophisticated equipment and infrastructure, complex multi-step and time consuming separation and purification processes of fission- $^{99}\text{Mo}$  in addition to generation of considerable amounts of radioactive wastes including intermediate- and long-lived fission-products [5]. Unfortunately,  $^{99}\text{Mo}$  supply reliability has been adversely affected over the past decade, causing a global shortage due to unexpected or extended shutdowns of some  $^{99}\text{Mo}$ -producing reactors and processing facilities [6], while the predicted annual growth of the baseline market is 3% [7].

Thus,  $(n, \gamma)^{99}\text{Mo}$  and the less-common cyclotron-produced  $^{99}\text{Mo}$  may represent alternatives of fission- $^{99}\text{Mo}$ , since such production routes are necessary to meet the global increasing demand. Although  $(n, \gamma)^{99}\text{Mo}$  has a lower specific activity (< 10 Ci/g) [8], it has many advantages where simple equipment is needed for processing, radionuclidic contamination is limited by the target purity (especially for  $^{98}\text{Mo}$  enriched targets) and the produced radioactive waste is minimal.

Neutron-activation  $^{99}\text{Mo}/^{99\text{m}}\text{Tc}$  generators include: (i) *chromatographic column generators* prepared either firstly by adsorption of  $^{99}\text{Mo}$  on high-capacity sorbents (such as polyzirconium compound, alumina functional-

\*Corresponding author: M. Mostafa, Radioactive Isotopes and Generators Dept., Hot Labs. Center, Atomic Energy Authority, P.O.B. 13759, Cairo, Egypt, e-mail: mmostafa95@yahoo.com

H. M. Saber, A. A. El-Sadek: Radioactive Isotopes and Generators Dept., Hot Labs. Center, Atomic Energy Authority, P.O.B. 13759, Cairo, Egypt

M. Y. Nassar: Chemistry Dept. Faculty of Science, Benha University, Benha 13518, Egypt

ized with sulfate moiety, polytitanium oxychloride and nanocrystalline  $\gamma$ - $\text{Al}_2\text{O}_3$  with capacities of 200–500 mg Mo/g) [4] or secondly by incorporation of Mo into gel materials [e.g., 12-molybdocerate, 6-tungstocerate, stannic molybdate, titanium molybdate, zirconium molybdate, zirconium molybdophosphate, alumina molybdate, cerium(IV) molybdate, cerium(IV) tellurium molybdate] via precipitation reactions using the post-irradiation method or the less-common pre-irradiation method [9–17], (ii) *Extraction generators* including solvent extraction (conventional or aqueous biphasic system), solid phase extraction generators, extraction chromatographic generators and supported liquid membrane generators (as a modified version of extraction chromatography) (iii) *sublimation and thermochromatographic generators* and (iv) *electrochemical generators* [4].

Gel generators are the most famous for  $(n, \gamma)^{99}\text{Mo}$ , especially those based on zirconium molybdate. Generally,  $^{99\text{m}}\text{Tc}$  is eluted from chromatographic column generators with 0.9% NaCl. Gel materials should contain a high content of Mo and  $^{99\text{m}}\text{Tc}$  should be eluted from them with a high yield within small volume of NaCl solution with specifications (Mo breakthrough, radiochemical and chemical purities and pH-value) meeting those of clinical grade according to pharmacopeias [4, 18].

## 2 Experimental

### 2.1 Chemical reagents

All the chemicals used in the present work were of AR grade. Distilled water was used for preparing solutions.

### 2.2 Instruments

Activity measurements were done by a gamma-ray spectrometer, which has a p-type coaxial HPGe detector (GX2518 model), Canberra, USA, with 29.4% relative efficiency and 1.66 keV FWHM at 1332.5 keV (of  $^{60}\text{Co}$ ). The detector is coupled with a multichannel analyzer (MCA), power supply and amplifier that are contained in one unit (Inspector 2000 model, Canberra Series, made in USA). Relative efficiency curve of the HPGe detector was obtained by using  $^{152,154}\text{Eu}$  point source. The absolute efficiency curve of the detector was obtained by using the standard point sources of  $^{137}\text{Cs}$  (S/N: C-145-8, Oxford) and  $^{60}\text{Co}$  (S/N: C-142-10, Oxford).

A pH-meter with a microprocessor (Hanna Instruments pH211 model, Portugal) was used for measuring pH-values of solutions.

An analytical balance (A&D Engineering Inc., AND HR-202 model, USA) having dual range (42 g/0.01 mg, 210 g/0.1 mg) was used for weighing.

X-ray diffraction was performed with an 18 kV diffractometer (Bruker, model D8 Advance, USA) with monochromated  $\text{Cu } K_{\alpha}$  radiation ( $\lambda = 1.54178 \text{ \AA}$ ).

Elemental analysis was carried out with X-ray fluorescence spectrometer (using Philips XRF, BW-1200 sequential spectrometer, Netherlands).

The morphology has been characterized using a field emission scanning electron microscope (FESEM) (JSM-6510A, Japan).

Surface area and pore size were determined by BET surface area and pore size analyzer (Quantachrome Nova 1000 E, USA).

The IR spectrum was recorded with an FT-IR spectrometer (Bomem, model MB157S, Canada) in the range from 4000 to 400  $\text{cm}^{-1}$  at room temperature.

Thermal analysis, including simultaneous TGA and DTA, was carried out with a thermal analyzer (Shimadzu, model DTG-60H, Japan).

Concentration of the possible chemical impurities in  $^{99\text{m}}\text{Tc}$  eluates was determined using inductively coupled plasma (ICP) spectrometer (sequential plasma emission spectrometer, ICPS-7500, Shimadzu, Japan).

### 2.3 Molybdenum-99 radiotracer

Molybdenum-99 was obtained by eluting commercial  $^{99}\text{Mo}/^{99\text{m}}\text{Tc}$  chromatographic column generators based on alumina (Mon-Tek Generator, Monrol Nuclear Products Industry and Trade Inc., Turkey). Each column was eluted, 20 d after the calibration date, with 20 mL of 2 M  $\text{NH}_3$  solution. Then, the  $\text{NH}_3$  solution was evaporated to dryness. The residual  $^{99}\text{Mo}$  was redissolved in 5 mL of 0.1 M NaOH to obtain the radiotracer solution. The  $^{99}\text{Mo}$  radiotracer solution contained 3.5 mCi  $^{99}\text{Mo}$ , i.e.,  $^{99}\text{Mo}$  activity concentration was 0.7 mCi/mL.

### 2.4 Preparation studies of zirconium molybdsilicate ( $\text{ZrMoSi}$ )

The effect of factors mentioned below on the (i)  $^{99}\text{Mo}$  precipitation yield (via  $\text{ZrMoSi}$  gel precipitation), (ii)  $^{99\text{m}}\text{Tc}$  elution yield and (iii)  $^{99}\text{Mo}$  breakthrough (in the eluate of the  $^{99}\text{Mo}/^{99\text{m}}\text{Tc}$  generator) was investigated.

## 2.5 Effect of pH-value along with drying temperature

50 mL of 0.25 M  $^{99}\text{Mo}(\text{VI})$  solution was prepared by dissolving 1.7992 g of  $\text{MoO}_3$  in 20 mL of 3 M NaOH and few drops of 5%  $\text{H}_2\text{O}_2$ , followed by addition of 5 mL of  $^{99}\text{Mo}$  radiotracer solution, 20 mL of 5%  $\text{H}_2\text{O}_2$ , concentrated  $\text{HNO}_3$  till pH 1, 2 or 3 and diluting the solution to 50 mL with 0.1, 0.01 or 0.001 M  $\text{HNO}_3$  to obtain a Mo(VI) solution of pH 1, 2 or 3, respectively. 50 mL of 0.25 M Si(IV) solution was prepared by dissolving 2.6517 g of  $\text{Na}_2\text{SiO}_3 \cdot 5\text{H}_2\text{O}$  in 30 mL  $\text{H}_2\text{O}$  and diluting to 50 mL with 5%  $\text{H}_2\text{O}_2$ . 50 mL of Zr(IV) solution was prepared by dissolving 4.0281 g of  $\text{ZrOCl}_2 \cdot 8\text{H}_2\text{O}$  in 30 mL  $\text{H}_2\text{O}$  and diluting to 50 mL with 5%  $\text{H}_2\text{O}_2$ .

Both of  $^{99}\text{Mo}(\text{VI})$  and Si(IV) solutions were simultaneously added dropwise to Zr(IV) solution with stirring to obtain a mixture solution of Zr : Mo : Si molar ratio of

1 : 1 : 1. After complete addition, pH of the mixture solution was adjusted again to 1, 2 or 3, according to the corresponding used  $^{99}\text{Mo}(\text{VI})$  solution, using  $\text{HNO}_3$ . The mixture was evaporated by heating on a hot plate. The gel material began to precipitate as  $\text{H}_2\text{O}_2$  decomposed. The heating continued till near dryness. Thereafter, the gel material was dried in an electric furnace at 100, 150 or 200 °C for 24 h (Table 1).

## 2.6 Effect of the molar ratio

The optimum pH and drying temperature were chosen for carrying out the study of the Zr : Mo : Si molar ratio effect. 100 mL of each of Mo(VI), Si(IV) and Zr(IV) was prepared as mentioned above, with duplication of the weights of the used reagents used in the case of 50 mL volumes. The mixing process was the same as mentioned above but

**Table 1:** Effect of pH and drying temperature on  $^{99}\text{Mo}$  precipitation yield (from 150 mL mixture solution),  $^{99\text{m}}\text{Tc}$  elution yield and  $^{99}\text{Mo}$  breakthrough in the eluate using Zr(IV) : Mo(VI) : Si(IV) molar ratio of 1 : 1 : 1.

pH	$^{99}\text{Mo}$ precipitation yield, %	$^{99\text{m}}\text{Tc}$ eluate in 10 mL of 0.9% NaCl solution	Drying temperature		
			100 °C	150 °C	200 °C
1	88.4	Average $^{99\text{m}}\text{Tc}$ elution yield $\pm \sigma^*$ , %	71 ± 2	62 ± 4	46 ± 5
		Average $^{99}\text{Mo}$ breakthrough $\pm \sigma$ , %	4 ± 1	2 ± 1	1.6 ± 0.6
2	93.4	Average $^{99\text{m}}\text{Tc}$ elution yield $\pm \sigma$ , %	73 ± 4	68 ± 3	63 ± 2
		Average $^{99}\text{Mo}$ breakthrough $\pm \sigma$ , %	$6 \times 10^{-3}$ $\pm 2 \times 10^{-3}$	$6 \times 10^{-3}$ $\pm 2 \times 10^{-3}$	$5 \times 10^{-3}$ $\pm 3 \times 10^{-3}$
3	75.3	Average $^{99\text{m}}\text{Tc}$ elution yield $\pm \sigma$ , %	70 ± 2	50 ± 4	36 ± 3
		Average $^{99}\text{Mo}$ breakthrough $\pm \sigma$ , %	5 ± 1	3 ± 1	3 ± 1

\*  $\sigma$ : standard deviation.

**Table 2:** Effect of Zr : Mo : Si molar ratio on  $^{99}\text{Mo}$  precipitation yield (from 60 mL mixture solution at pH 2),  $^{99\text{m}}\text{Tc}$  elution yield and  $^{99}\text{Mo}$  breakthrough in the eluate at drying temperature of 100 °C.

Mixture no.	Volume, mL				Molar ratio (Zr : Mo : Si)	$^{99}\text{Mo}$ precipitation yield, %	$^{99\text{m}}\text{Tc}$ eluate in 0.9% NaCl solution	
	Zr(IV) solution	Mo(VI) solution	Si(IV) solution	$\text{H}_2\text{O}$			Average $^{99\text{m}}\text{Tc}$ elution yield $\pm \sigma$ , %	Average $^{99}\text{Mo}$ breakthrough $\pm \sigma$ , %
1	20 mL	20 mL	20 mL	0 mL	1 : 1 : 1	94.1	73 ± 3	$6 \times 10^{-3} \pm 1 \times 10^{-3}$
2	10 mL	10 mL	20 mL	20 mL	0.5 : 0.5 : 1	97.9	82 ± 2	$1.0 \times 10^{-3} \pm 0.6 \times 10^{-3}$
3	10 mL	20 mL	10 mL	20 mL	0.5 : 1 : 0.5	90.5	74 ± 3	1.6 ± 0.4
4	15 mL	15 mL	20 mL	10 mL	0.75 : 0.75 : 1	97.7	67 ± 3	$2 \times 10^{-3} \pm 1 \times 10^{-3}$
5	15 mL	20 mL	15 mL	10 mL	0.75 : 1 : 0.75	91.6	76 ± 2	0.2 ± 0.1
6	20 mL	15 mL	15 mL	10 mL	1 : 0.75 : 0.75	93.2	46 ± 5	ND

with using different volumes from each solution to obtain different molar ratios, but the final volume of the mixture solution in each case was 60 mL. Zr : Mo : Si molar ratios of 1 : 1 : 1, 0.5 : 0.5 : 1, 0.5 : 1 : 0.5, 0.75 : 0.75 : 1, 0.75 : 1 : 0.75 and 1 : 0.75 : 0.75 were studied (Table 2).

## 2.7 Preparation of $^{99}\text{Mo}/^{99\text{m}}\text{Tc}$ chromatographic column generators

A 0.7 cm ID glass column was used for each  $^{99}\text{Mo}/^{99\text{m}}\text{Tc}$  generator. Each column was provided with a small piece of glass wool, as a support for the gel bed, and a bottom stopcock. The dried gel was gently pulverized with a glass rod. 1.3 g of the pulverized ZrMoSi gel bed was packed into the column by settling from distilled water. The suspended fine particles, in case of their presence, were withdrawn (with a hose and syringe). The column was excessively washed with distilled water and subsequently conditioned with 50 mL of 0.9% NaCl for further elution of  $^{99\text{m}}\text{Tc}$ . The gel particles were further disintegrated by the action of NaCl during the conditioning step.

## 2.8 $^{99}\text{Mo}$ precipitation yield

Molybdenum-99 precipitation yield,  $Y_p$ , was calculated according to the following equation:

$$Y_p = \frac{\text{Mo}C_0 \times V_r - \text{Mo}C_f \times V_w}{\text{Mo}C_0 \times V_r \times e^{-\lambda t}} \times 100 \quad (1)$$

where:

- $\text{Mo}C_0$  and  $\text{Mo}C_f$ : are the count rates of 10  $\mu\text{L}$  of the  $^{99}\text{Mo}$  radiotracer solution and water washing effluent of the prepared generators, respectively.
- $V_r$  and  $V_w$ : are the volumes of the radiotracer solution and water washing effluent (mL), respectively.
- $\lambda$ : is the decay constant of  $^{99}\text{Mo}$  ( $0.252 \text{ d}^{-1}$ ).
- $t$ : is the time elapsed from the beginning of gel preparation to the count time (d).

## 2.9 Performance of $^{99}\text{Mo}/^{99\text{m}}\text{Tc}$ generator

Technetium-99m was firstly eluted 23 h after the conditioning time by passing 10 mL of 0.9% NaCl solution through the ZrMoSi gel column. The column was eluted 14 times over the course of 21 days. The time between each two successive elutions was  $\geq 23$  h. The  $^{99\text{m}}\text{Tc}$  elution

yield,  $Y_e$ , was determined by using the following equation:

$$Y_e = \frac{\text{Tc}C_0 - \text{Tc}C_f}{\text{Tc}C_0} \times 100 (\%) \quad (2)$$

where:

- $\text{Tc}C_0$  and  $\text{Tc}C_f$ : are the count rates of the 140-keV peak in the  $\gamma$ -ray spectrum of the column directly before and after elution, taking the contribution of  $^{99}\text{Mo}$  to this peak into account [19].

The elution profiles were drawn as a function of elution flow rates. pH-values of  $^{99\text{m}}\text{Tc}$  eluates were determined using the pH-meter.

$^{99}\text{Mo}$  breakthrough in the eluate was determined as the percent contribution of the  $^{99}\text{Mo}$  activity to the total activity of the eluate. The  $\gamma$ -ray spectrum of the eluate was measured directly after elution and after 5 days to ensure the accurate  $^{99}\text{Mo}$  determination.

The radiochemical purity of the  $^{99\text{m}}\text{Tc}$  eluate (percent contribution of  $^{99\text{m}}\text{TcO}_4^-$  count rate to the total eluate count rate) was determined by ascending paper chromatography using Whatman no. 1 chromatographic paper and a mixture of 85% methanol + 15%  $\text{H}_2\text{O}$  as a developing solvent. The activity distribution along the chromatogram was determined using the  $\gamma$ -ray spectrometer to calculate  $R_f$ -value. This chromatographic method gives  $R_f$ -value of 0.55–0.7 for  $^{99\text{m}}\text{TcO}_4^-$  [20].

The possible Zr, Mo and Si impurities in  $^{99\text{m}}\text{Tc}$  eluate were determined by using the ICP at wavelengths of 343.823, 202.03 and 251.611 nm, respectively [21].

## 2.10 Characterization of ZrMoSi gel

The ZrMoSi gel prepared with the optimum conditions, without including  $^{99}\text{Mo}$  radiotracer, was characterized by BET surface area and pore size analyzer, IR spectroscopy, thermal analysis (TGA and DTA), XRD, XRF and FESEM.

## 3 Results and discussion

The Zr(IV), Mo(VI) and Si(IV) solutions used to prepare ZrMoSi gel contained excess of  $\text{H}_2\text{O}_2$ . Zirconium oxychloride interacts with excess  $\text{H}_2\text{O}_2$  forming  $\text{H}_6\text{ZrO}_6\text{Cl}_{2(\text{aq})}$  [22]. In  $\text{H}_2\text{O}_2$  solutions with a pH-value in the range of 1.6–2.5, Mo(VI) may form species such as  $[\text{MoO(OH)(O}_2]_{2(\text{aq})}^-$  while those of a pH-value in the range of 0.5–5 may contain species such as  $[\text{MoO}_3(\text{O}_2)]_{(\text{aq})}^{2-}$  [23]. The  $\text{HOOSiO}_2^-$  anion may be present in  $\text{H}_2\text{O}_2$  solution of  $\text{Na}_2\text{SiO}_3$  [24]. The used peroxy route is

advantageous for permitting a gradual precipitation of the gel material from Zr(IV)-Mo(VI)-Si(IV) mixture solution as  $\text{H}_2\text{O}_2$  and the formed peroxy species gradually decomposed and avoiding the need for filtration or centrifugation when the heating process continues to dryness [25]. In addition, the excess  $\text{H}_2\text{O}_2$  ensures the presence of  $^{99}\text{Mo}$  in the hexavalent state.

### 3.1 $^{99}\text{Mo}$ precipitation yield, $^{99\text{m}}\text{Tc}$ elution yield and $^{99}\text{Mo}$ breakthrough

According to Table 1, with Zr : Mo : Si molar ratio of 1 : 1 : 1, the highest  $^{99}\text{Mo}$  precipitation yield was achieved at pH 2. The highest  $^{99\text{m}}\text{Tc}$  elution yield was achieved also with the gel precipitated at pH 2 and dried at 100 °C. The lowest  $^{99}\text{Mo}$  breakthrough was achieved at pH 2 and drying temperature of 200 °C, which was only slightly lower than that achieved at 100 °C. Thus pH 2 and drying temperature of 100 °C were chosen for the further molar ratio study. Comparing the values of  $^{99}\text{Mo}$  precipitation yield,  $^{99\text{m}}\text{Tc}$  elution yield and  $^{99}\text{Mo}$  breakthrough for gel materials precipitated at pH 2 with Zr : Mo : Si molar ratio of 1 : 1 : 1 from 150 and 60 mL mixture solution and dried at 100 °C (Tables 1 and 2), one can conclude that variation of the mixture solution volume had not a significant effect on the prementioned values. According to Table 2, the highest  $^{99}\text{Mo}$  precipitation yield and the highest  $^{99\text{m}}\text{Tc}$  elution yield were achieved with the Zr : Mo : Si molar ratio of 0.5 : 0.5 : 1 (with an acceptable  $^{99}\text{Mo}$  breakthrough for medical uses [26]), and thus it was chosen for the further gel characterization and the other specifications of  $^{99}\text{Mo}/^{99\text{m}}\text{Tc}$  column generator performance ( $^{99\text{m}}\text{Tc}$  elution profiles as a function of flow rate, pH-value of the eluate, radiochemical purity and chemical purity).

### 3.2 Characterization of the ZrMoSi gel prepared with the optimum conditions

ZrMoSi gel precipitated at pH 2 from a mixture solution with Zr : Mo : Si molar ratio of 0.5 : 0.5 : 1 and dried at 100 °C was characterized. This gel material was granular and white to pale yellow colored. Table 3 compiles some physical characteristics of ZrMoSi gel prepared at the optimum conditions. According to Table 3, ZrMoSi gel material is a microporous material with an average pore size of 1.39 nm [27], an average particle size of 0.73 mm and a specific surface area of 14.28  $\text{m}^2/\text{g}$ .

Figure 1 shows the IR spectrum of the prepared ZrMoSi gel. The band at  $472 \text{ cm}^{-1}$  may be assigned to  $\text{SiMo}_{12}$  clus-

**Table 3:** Some physical characteristics of ZrMoSi gel precipitated at pH 2 from 150 mL mixture solution with Zr(IV) : Mo(VI) : Si(IV) molar ratio of 0.5 : 0.5 : 1 and dried at 100 °C.

Appearance	Granular
Color	White-pale yellow
Specific surface area*	14.28 $\text{m}^2/\text{g}$
Total pore volume*	$9.89 \times 10^{-3} \text{ cc/g}$
Average pore size*	1.39 nm
Average particle size**	0.73 mm

\* Determined from BET.

\*\* Determined from FESEM images.

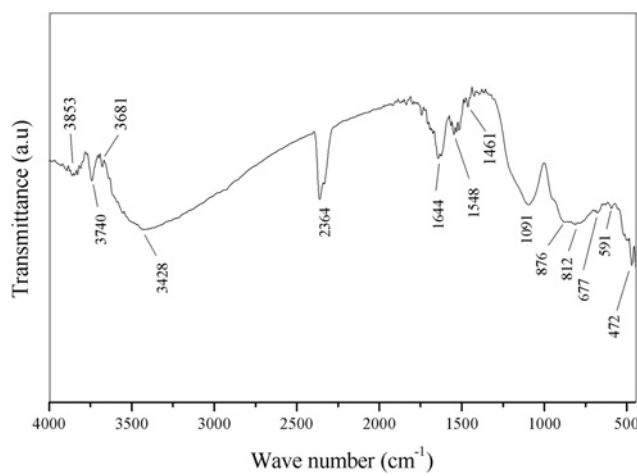


**Fig. 1:** IR spectrum of ZrMoSi gel.

ter [28–31]. The bands at 591, 812, 876 and 1091  $\text{cm}^{-1}$  may be assigned to different M–O bonds (M = Zr, Mo or Si). The band at 677  $\text{cm}^{-1}$  may be assigned to vibrations associated with defects as neutral oxygen vacancies (described as  $\equiv\text{Si}-\text{Si}\equiv$ ) [32]. The bands at 1461 and 1548  $\text{cm}^{-1}$  may be attributed to deformation vibrations of metal hydroxyl groups [33]. The bands at 1644 and 3428  $\text{cm}^{-1}$  may be assigned to O–H bending and stretching vibration modes of lattice water, respectively [34, 35]. The band at 2364  $\text{cm}^{-1}$  may be related to  $\text{CO}_2$  adsorbed from the environment [36, 37]. The bands at 3681, 3740 and 3853  $\text{cm}^{-1}$  may be assigned to Si–OH and Zr–OH bonds [38–42].

Figure 2 shows TGA and DTA curves of ZrMoSi gel. There was a weight loss of 13.9% in the temperature range from 40 to 311 °C due to the loss of physical adsorbed and lattice water. An exothermic peak was observed at 62 °C followed by an endothermic one at 78 °C. A shallow broad endothermic peak was observed at 244 °C. The presence of lattice water with a suitable amount in the gel material facilitates the eluent diffusion [43]. There was only a small weight loss of 1.3%, in the temperature range of

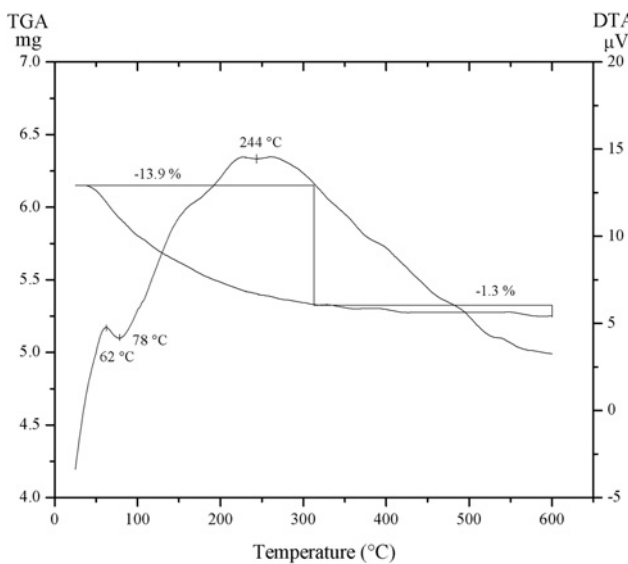


**Fig. 2:** TGA and DTA curves of ZrMoSi gel.

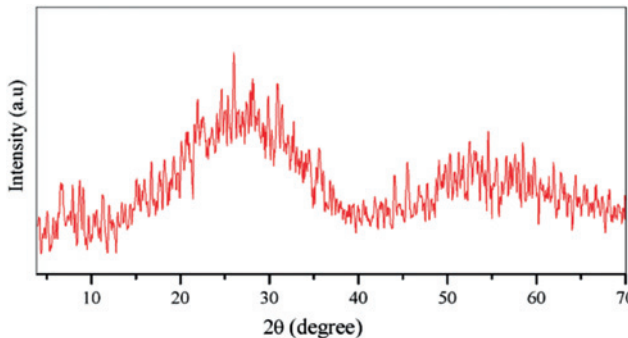


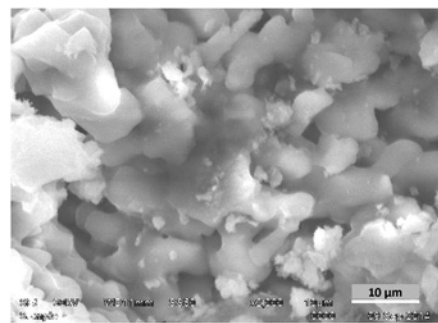
**Fig. 3:** XRD pattern of ZrMoSi gel.

338–600 °C, may be due to loss of the structural water by slow diffusion from gel interior [44–47].

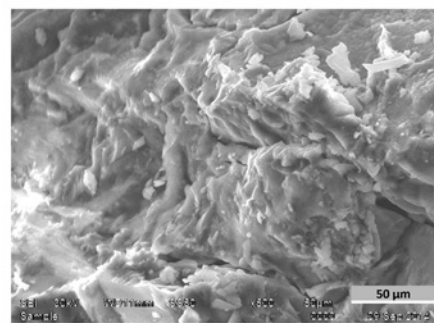
Figure 3 shows the XRD pattern of ZrMoSi gel, which indicates its amorphous structure. Generally, the amorphous structure is advantageous over the rigid crystal structure, where the former permits better diffusion of the eluent through the bed material of  $^{99}\text{Mo}/^{99\text{m}}\text{Tc}$  generator leading to a higher elution yield of  $^{99\text{m}}\text{Tc}$ . In the same time, the amorphous structure is more resistant to dissolution which results in  $^{99\text{m}}\text{Tc}$  eluates of higher chemical purity [13].

XRF measurements revealed that Zr : Mo : Si molar ratio in the prepared ZrMoSi gel was 0.5 : 0.6 : 1 which was nearly the same as in the mixture solution used for preparation (0.5 : 0.5 : 1).

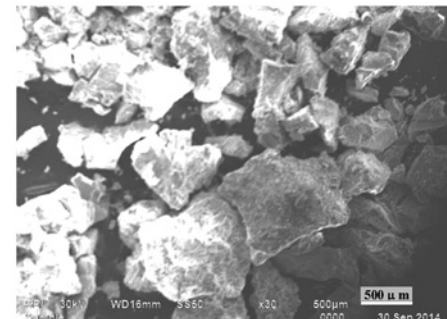
Figure 4 shows FESEM images of ZrMoSi, which indicates jelly-like entangled pieces with many meanders through which the saline eluent can diffuse.



(a)



(b)



(c)

**Fig. 4:** FESEM images of ZrMoSi gel.

### 3.3 Performance of the $^{99}\text{Mo}/^{99\text{m}}\text{Tc}$ generator

The generator based on ZrMoSi gel prepared with the optimum conditions was thoroughly investigated. As mentioned above, the elution yield was 82% and the  $^{99}\text{Mo}$  breakthrough was  $1.0 \times 10^{-3}\%$ . Figure 5 shows elution profiles of  $^{99\text{m}}\text{Tc}$  from ZrMoSi gel as a function of flow rate. Sharp elution profiles were obtained with the flow rates of 0.4, 1.2 and 1.5 mL/min with maxima at the 1<sup>st</sup> mL of eluate containing 63.9, 56.7 and 46.4% of the total

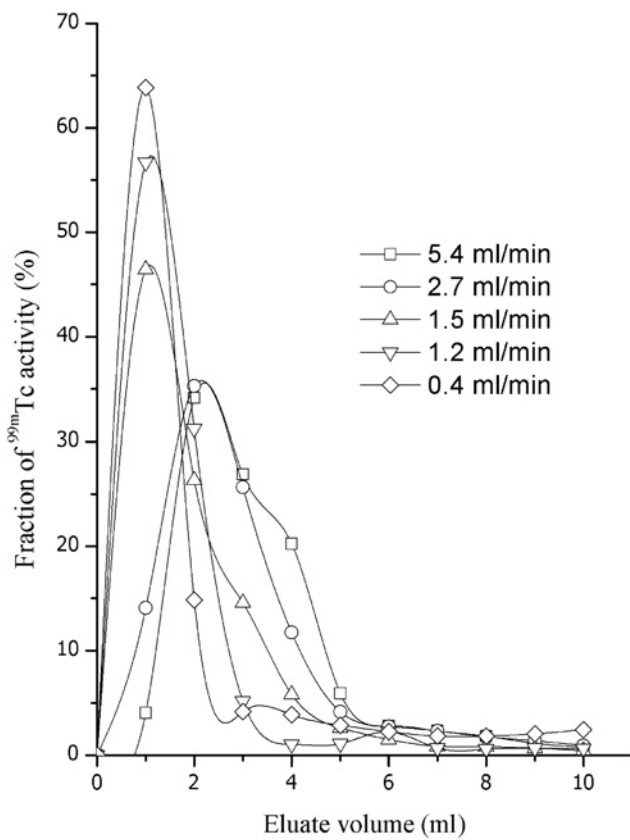


**Fig. 5:** Elution profiles of  $^{99\text{m}}\text{Tc}$  from  $\text{Zr}^{99}\text{MoSi}$  gel column generator as a function of flow rate.

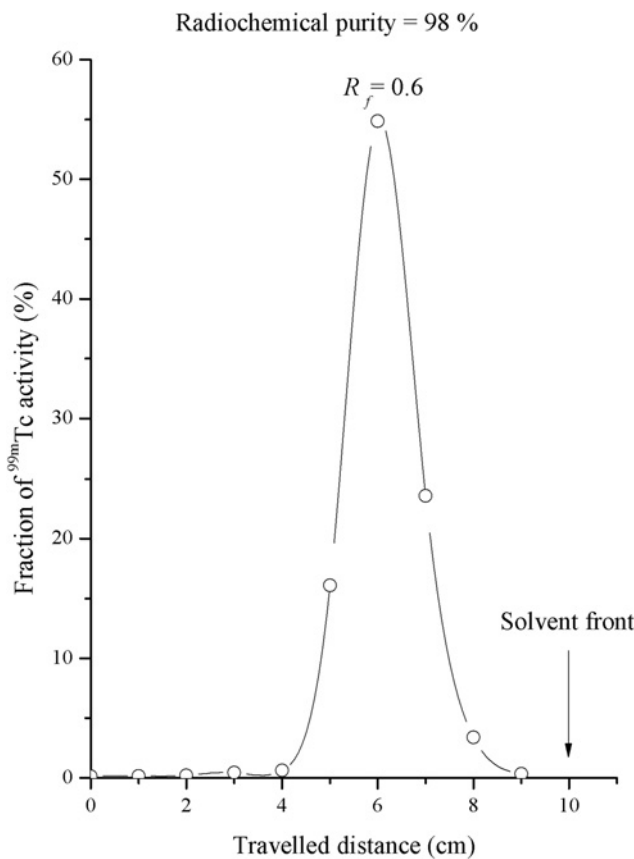
$^{99\text{m}}\text{Tc}$  eluted activity, respectively. Broader profiles were obtained with the flow rates of 2.7 and 5.4 mL/min with maxima at the 2<sup>nd</sup> mL of eluate containing 35.3 and 34.1% of the total  $^{99\text{m}}\text{Tc}$  eluted activity, respectively. The pH-value of the eluate ranged from 5.5–7.

Figure 6 shows the radiochromatogram of the eluted  $^{99\text{m}}\text{Tc}$  using the ascending paper chromatography. A single peak was obtained with  $R_f$  value of 0.6, characteristic of  $^{99\text{m}}\text{TcO}_4^-$ . Radiochemical purity (area under  $R_f$ -peak) was found to be 98%. Table 4 compiles the detailed  $^{99\text{m}}\text{Tc}$  elution yield,  $^{99}\text{Mo}$  breakthrough and radiochemical purity for the  $^{99}\text{Mo}/^{99\text{m}}\text{Tc}$  column packed with  $\text{ZrMoSi}$  gel prepared with the optimum conditions.

Zr and Si impurities were not detected in  $^{99\text{m}}\text{Tc}$  eluates, while Mo levels in the  $^{99\text{m}}\text{Tc}$  eluates were found to be  $\leq 0.4$  ppm, which are less than the permitted parenteral Mo concentration [48].

## 4 Conclusion

$\text{ZrMoSi}$  gel was prepared, characterized and used successfully as a base material for  $^{99}\text{Mo}/^{99\text{m}}\text{Tc}$  column generator.



**Fig. 6:** Radiochromatogram of  $^{99\text{m}}\text{Tc}$  eluted from  $\text{Zr}^{99}\text{MoSi}$  gel column generator, using Whatman no. 1 ascending paper chromatographic method and 85% methanol as a developing solvent.

**Table 4:** Detailed  $^{99\text{m}}\text{Tc}$  elution yield,  $^{99}\text{Mo}$  breakthrough and radiochemical purity for the  $^{99}\text{Mo}/^{99\text{m}}\text{Tc}$  column packed with  $\text{ZrMoSi}$  gel ( $\text{Zr} : \text{Mo} : \text{Si}$  molar ratio of 0.5 : 0.5 : 1) precipitated at pH 2 and dried at 100 °C.

Elution day	$^{99\text{m}}\text{Tc}$ elution yield, %	$^{99}\text{Mo}$ breakthrough, %	Radiochemical purity (as $^{99\text{m}}\text{TcO}_4^{2-}$ ), %
1	81	$9 \times 10^{-4}$	98
2	79	$2 \times 10^{-3}$	
3	80	$2 \times 10^{-3}$	99
4	82	$1 \times 10^{-3}$	
7	80	$1 \times 10^{-3}$	
8	85	$8 \times 10^{-4}$	97
9	86	$5 \times 10^{-4}$	
11	82	$1 \times 10^{-3}$	98
14	83	$7 \times 10^{-4}$	
15	83	$9 \times 10^{-4}$	
16	82	$4 \times 10^{-4}$	98
17	84	$5 \times 10^{-4}$	
18	83	$2 \times 10^{-3}$	
21	84	$8 \times 10^{-5}$	98
Average $\pm \sigma$	$82 \pm 2$	$1.0 \times 10^{-3} \pm 0.6 \times 10^{-3}$	$98 \pm 1$

Precipitating the gel material at pH 2 with Zr : Mo : Si molar ratio of 0.5 : 0.5 : 1 and drying it at 100 °C for 24 h resulted in the optimum performance of the prepared generator. The specifications of the eluted  $^{99\text{m}}\text{Tc}$  met the requirements of the medical use. Future studies will be carried out for preparation of ZrMoSi gel using neutron-irradiated molybdenum (instead of fission  $^{99}\text{Mo}$  radiotracer) to produce higher activity  $^{99}\text{Mo}/^{99\text{m}}\text{Tc}$  generators ( $\geq 1 \text{ Ci}$ ). Such future studies are necessary to be sure if the performance of the generator will be changed (by using higher  $^{99}\text{Mo}$  activities) or not and, hence, to see if any modification in the preparation conditions will be needed.

## References

- Bryan, R. N.: *Introduction to the Science of medical Imaging*, Cambridge University Press, New York 2010.
- Guérin, B., Tremblay, S., Rodrigue, S., Rousseau, J. A., Dumulon-Perreault, V., Lecomte, R., van Lier, J. E., Zyuzin, A., van Lier, E. J.: Cyclotron production of  $^{99\text{m}}\text{Tc}$ : an approach to the medical isotope crisis. *J. Nucl. Med.* **51**, 13N (2010).
- Arino, H., Kramer, H. H.: Fission product  $^{99\text{m}}\text{Tc}$  generator. *Int. J. Appl. Radiat. Isot.* **26**, 301 (1975).
- Dash, A., Knapp, F. R., Pillai, M.:  $^{99}\text{Mo}/^{99\text{m}}\text{Tc}$  separation: An assessment of technology options. *Nucl. Med. Biol.* **40**, 167 (2013).
- IAEA (International Atomic Energy Agency): Fission molybdenum for medical use. IAEA-TECDOC-515 (1989).
- OECD (Organisation for Economic Co-operation and Development): Medical isotope supply in the future: Production capacity and demand forecast for the  $^{99}\text{Mo}/^{99\text{m}}\text{Tc}$  market, 2015–2020. NEA/SEN/HLGMR (2014).
- Frontera, M., Bernstein, A., Eriksson, T., Figon, M., Granath, K., Orbe, M., Shanks, C., Stromqvist, E., Woodland, J., Zavodszky, P.: Future supply options of  $^{99}\text{Mo}$  and  $^{99\text{m}}\text{Tc}$ . Mo-99 2014 Topical Meeting on Molybdenum-99 Technological Development. 24–27 June, Washington DC (2014).
- Zolle, I.: Technetium-99m Pharmaceuticals: Preparation and Quality Control in Nuclear Medicine, Springer, Berlin (2007).
- El-Absy, M., El-Bayoumy, S.: The use of stannic molybdate- $^{99}\text{Mo}$  as a  $^{99\text{m}}\text{Tc}$ -generator. *Isotopen Praxis* **26**, 60 (1990).
- El-Kolaly, M.: A  $^{99}\text{Mo}/^{99\text{m}}\text{Tc}$  generator based on the use of zirconium molybdochosphate- $^{99}\text{Mo}$  gel. *J. Radioanal. Nucl. Chem.* **170**, 293 (1993).
- El-Absy, M., El-Enein, M. A., Raieh, M., Aly, H.: Isotope exchange between 12-molybdocerate(IV) and sodium molybdate- $^{99}\text{Mo}$  in aqueous media. *J. Radioanal. Nucl. Chem.* **218**, 157 (1997).
- Monroy-Guzman, F., Romero, O. C., Velázquez, H. D.: Titanium molybdate gels as matrix of  $^{99}\text{Mo}/^{99\text{m}}\text{Tc}$  generators. *J. Nucl. Radiochem. Sci.* **8**, 11 (2007).
- Monroy-Guzman, F., Díaz-Archundia, L. V., Hernández-Cortés, S.:  $^{99}\text{Mo}/^{99\text{m}}\text{Tc}$  generators performances prepared from zirconium molybdate gels. *J. Braz. Chem. Soc.* **19**, 380 (2008).
- Mostafa, M., El-Sadek, A., El-Said, H., El-Amir, M.:  $^{99}\text{Mo}/^{99\text{m}}\text{Tc}$  –  $^{113}\text{Sn}/^{113\text{m}}\text{In}$  dual radioisotope generator based on 6-tungstocerate(IV) column matrix. *J. Nucl. Radiochem. Sci.* **10**, 1 (2009).
- Mostafa, M., Ramadan, H., El-Amir, M., El-Said, H.:  $^{99}\text{Mo}/^{99\text{m}}\text{Tc}$  chromatographic column generator based on cerium(IV) molybdate gel. *Radiochemistry* **55**, 332 (2013).
- El-Absy, M., El-Amir, M., Fasih, T., Ramadan, H., El-Shahat, M.: Preparation of  $^{99}\text{Mo}/^{99\text{m}}\text{Tc}$  generator based on alumina  $^{99}\text{Mo}$ -molybdate (VI) gel. *J. Radioanal. Nucl. Chem.* **299**, 1859 (2014).
- El-Amir, M., Mostafa, M., Ramadan, H.: Preparation and characterization of cerium(IV) tellurium molybdate gel and its application as a bed for chromatographic  $^{99}\text{Mo}/^{99\text{m}}\text{Tc}$  generator. *J. Nucl. Radiochem. Sci.* **14**, 1 (2014).
- Ishitsuka, E., Ishihara, M., Suzuki, M.: Proceedings of the Specialist Meeting on Mo-99 Production by ( $n, \gamma$ ) Method. March 9–10, Yurakucho Asahi Hall, Tokyo (2012).
- Simonits, A., Moens, L., De Corte, F., De Wispelaere, A., Hoste, J.: Absolute intensity of the 140.5 keV gamma-ray of  $^{99}\text{Mo}$ . *J. Radioanal. Chem.* **67**, 61 (1981).
- IAEA (International Atomic Energy Agency): Technetium-99m radiopharmaceuticals: Manufacture of kits. Technical Reports Series No. 466, Vienna (2008).
- Schierle, C., Otto, M.: Qualitative and semi-quantitative analysis in ICP-AES using multivariate calibration. *Mikrochim. Acta* **113**, 357 (1994).
- Young, D. A., Linda, Y.: Crystalline titanosilicate zeolites. US Pat. No. 3,329,481 (1967).
- Campbell, N. J., Dengel, A. C., Edwards, C. J., Griffith, W. P.: Studies on transition metal peroxy complexes. Part 8. The nature of peroxyomolybdates and peroxtungstates in aqueous solution. *J. Chem. Soc. Dalton trans.* **1989**, 1203 (1989).
- Lobachev, V., Savelova, V., Prokop'eva, T.: Catalysis by hydrogen carbonate and silicate anions of the oxidation of diethyl sulfide with hydrogen peroxide in aqueous and aqueous alcoholic media. *Theor. Exp. Chem.* **40**, 161 (2004).
- Liang, Q.: Development and optimization of W-88/Re188 and Mo-99/Tc-99m gel radioisotope generators. PhD Thesis, Missouri University, Columbia, USA (1996).
- Saha, G. B.: *Fundamentals of Nuclear Pharmacy*, 6<sup>th</sup> ed., Springer, Berlin 2010.
- Mohamed, M. H., Wilson, L. D.: Porous copolymer resins: Tuning pore structure and surface area with non reactive porogens. *Nanomater.* **2**, 163 (2012).
- Rocchiccioli-Deltcheff, C., Amiroche, M., Fournier, M.: Structure and catalytic properties of silica-supported polyoxomolybdates III. 12-molybdosilicic acid catalysts: Vibrational study of the dispersion effect and nature of the Mo species in interaction with the silica support. *J. Catal.* **138**, 445 (1992).
- Sohn, J. R., Chun, E. W., Pae, Y. I.: Spectroscopic studies on  $\text{ZrO}_2$  modified with  $\text{MoO}_3$  and activity for acid catalysis. *Bull. Korean Chem. Soc.* **24**, 1785 (2003).
- Cavalu, S., Banica, F.: Surface modification of alumina/zirconia ceramics upon different fluoride-based treatments. *Int. J. Appl. Ceram. Technol.* **11**, 402 (2014).
- Byrapa, K., Kumar, S.: Characterization of zeolites by infrared spectroscopy. *Asian Journal of Chemistry* **19**, 4933 (2007).
- Luna-López, J. A., Carrillo-López, J., Aceves-Mijares, M., Morales-Sánchez, A., Falcony, C.: FTIR and photoluminescence of annealed silicon rich oxide films. *Superficies y Vacío* **22**, 11 (2009).

33. Sharma, H. K., Sharma, N.: Synthesis and structural characterization of tin (IV) molybdate-A heteropolyacid salt. *Der Chemica Sinica* **4**, 182 (2013).
34. Srivastava, S. K., Singh, R. P., Agrawal, S., Kumar, S.: Synthesis and ion-exchange properties of cerium(IV) molybdate. *J. Radioanal. Nucl. Chem.* **40**, 7 (1977).
35. Moffat, J. B.: Metal-oxygen clusters: *The surface and catalytic properties of heteropoly oxometalates*, Kluwer Academic Publishers, New York 2002.
36. Walker, N. R., Walters, R. S., Grieves, G. A., Duncan, M. A.: Growth dynamics and intracluster reactions in  $\text{Ni}^+(\text{CO}_2)_n$  complexes via infrared spectroscopy. *J. Chem. Phys.* **121**, 10489 (2004).
37. da Conceicao, T. F., Scharnagl, N., Blawert, C., Dietzel, W., Kainer, K. U.: Surface modification of magnesium alloy AZ31 by hydrofluoric acid treatment and its effect on the corrosion behavior. *Thin Solid Films* **518**, 5209 (2010).
38. Chukin, G. D., Malevich, V. I.: Infrared spectra of silica. *J. Appl. Spectrosc.* **26**, 223 (1977).
39. Lenza, R. F. S., Vasconcelos, W. L.: Preparation of silica by sol-gel method using formamide. *Mater Res* **4**, 189 (2001).
40. Innocenzi, P.: Infrared spectroscopy of sol-gel derived silica-based films: a spectra-microstructure overview. *J. Non-Cryst. Solids* **316**, 309 (2003).
41. Gupta, P., Dillon, A. C., Coon, P. A., George, S. M.: FTIR studies reveal that silicon-containing laser-induced desorption products are surface reaction intermediates. *Chem Phys Lett* **176**, 128 (1991).
42. Davis, L. E., Bonini, N. A., Locatelli, S., Gonzo, E. E.: Characterization and catalytic activity of zirconium dioxide prepared by sol-gel. *Latin Am. Appl. Res.* **35**, 23 (2005).
43. Davarpanah, M. R., Nosrati, S. A., Fazlali, M., Boudani, M. K., Khoshhosn, H., Maragheh, M. G.: Influence of drying conditions of zirconium molybdate gel on performance of  $^{99\text{m}}\text{Tc}$  gel generator. *Appl. Radiat. Isot.* **67**, 1796 (2009).
44. Bardin, B. B., Bordawekar, S. V., Neurock, M., Davis, R. J.: Acidity of keggin-type heteropolycompounds evaluated by catalytic probe reactions, sorption microcalorimetry, and density functional quantum chemical calculations. *J. Phys. Chem. B* **102**, 10817 (1998).
45. Gimblett, G., Rahman, A. A., Sing, K. S. W.: Thermal and related studies of some zirconia gels. *J. Chem. Tech. Biotechnol.* **30**, 51 (1980).
46. Neves, G. M., Lenza, R. F. S., Vasconcelos, W. L.: Evaluation of the influence of microwaves in the structure of silica gels. *Mater. Res.* **5**, 447 (2002).
47. Wittoon, T., Chareonpanich, M.: Effect of pore size and surface chemistry of porous silica on  $\text{CO}_2$  adsorption. *Songklanakarin, J. Sci. Technol.* **34**, 403 (2012).
48. USP (US Pharmacopeia): Elemental Impurities, Standards-Setting Record (2012).